ORIGINAL ARTICLE

Reduced TET2 function leads to T-cell lymphoma with follicular helper T-cell-like features in mice

H Muto[1,2], M Sakata-Yanagimoto[1,2,3], G Nagae[4], Y Shiozawa[5], Y Miyake[2], K Yoshida[5], T Enami[2], Y Kamada[2], T Kato[2,3,6], K Uchida[7], T Nanmoku[8], N Obara[1,2,3], K Suzukawa[1,2,3,8], M Sanada[5], N Nakamura[9], H Aburatani[4], S Ogawa[5] and S Chiba[1,2,3,6]

TET2 (Ten Eleven Translocation 2) is a dioxygenase that converts methylcytosine (mC) to hydroxymethylcytosine (hmC). *TET2* loss-of-function mutations are highly frequent in subtypes of T-cell lymphoma that harbor follicular helper T (Tfh)-cell-like features, such as angioimmunoblastic T-cell lymphoma (30–83%) or peripheral T-cell lymphoma, not otherwise specified (10–49%), as well as myeloid malignancies. Here, we show that middle-aged *Tet2* knockdown (*Tet2*[gt/gt]) mice exhibit Tfh-like cell overproduction in the spleen compared with control mice. The *Tet2* knockdown mice eventually develop T-cell lymphoma with Tfh-like features after a long latency (median 67 weeks). Transcriptome analysis revealed that these lymphoma cells had Tfh-like gene expression patterns when compared with splenic CD4-positive cells of wild-type mice. The lymphoma cells showed lower hmC densities around the transcription start site (TSS) and higher mC densities at the regions of the TSS, gene body and CpG islands. These epigenetic changes, seen in *Tet2* insufficiency-triggered lymphoma, possibly contributed to predated outgrowth of Tfh-like cells and subsequent lymphomagenesis. The mouse model described here suggests that *TET2* mutations play a major role in the development of T-cell lymphoma with Tfh-like features in humans.

Blood Cancer Journal (2014) **4**, e264; doi:10.1038/bcj.2014.83; published online 12 December 2014

INTRODUCTION

In mammalian cells, three TET (Ten Eleven Translocation) proteins, TET1, TET2 and TET3, function as methylcytosine dioxygenases, commonly converting methylcytosine (mC) to hydroxymethylcytosine (hmC), which is thought to be an essential intermediate in both active and passive demethylation processes.[1,2] Furthermore, hmC is also believed to serve as an alternative epigenetic mark to mC in the regulation of gene expression.[3,4] Nevertheless, its biological function remains unclear.[5]

TET2 mutations are frequently found in myeloid malignancies (myelodysplastic syndromes, 14–26%; myeloproliferative neoplasm, 7.6–37% and acute myeloid leukemias, 12–43%).[6–9] *TET2* loss-of-function mutations are associated with aberrant DNA methylation patterns in myeloid malignancies.[10,11] Of interest here, *TET2* mutations are extremely frequent in subtypes of T-cell lymphoma such as angioimmunoblastic T-cell lymphoma (AITL, 30–83%) and peripheral T-cell lymphoma, not otherwise specified (PTCL-NOS, 10–49%).[12–14] AITL is thought to emerge from follicular helper T (Tfh) cells, based on findings from gene-expression profiling and immunohistochemical staining.[15,16] Tfh cells exist in the follicles of lymph nodes and spleen, and interact with follicular B cells and antigen-presenting cells.[17,18] *B-cell leukemia/lymphoma 6* (*Bcl6*) and *v-maf avian musculoaponeurotic fibrosarcoma oncogene homolog* (*cMaf*) encode key transcription factors governing Tfh differentiation and proliferation.[19] Tfh cells express co-stimulatory molecules such as programmed cell death

1 (PD1) and inducible T-cell costimulator (Icos),[20] as well as chemokine receptors, such as chemokine (C-X-C motif) receptor 5 (Cxcr5) on the cell surface.[21–25] PTCL-NOS is a group of heterogeneous T-cell lymphomas, some of which also show Tfh-like features.

Thus far, *Tet2* function has been assessed in various knockout/knockdown mice. Common phenotypes seen following *Tet2* loss are increased frequency of the lineage-negative, Sca1-positive and c-Kit-positive (LSK) fraction, enhanced competitive repopulation capacity and skewed differentiation toward myeloid lineages.[14,26–30] Some *Tet2*-knockout mice are reported to develop myeloid malignancies, resembling chronic myelomonocytic leukemia (CMML).[14,26,27]

Here, we show that *Tet2*-knockdown mice develop T-cell lymphoma with Tfh-like features. Comprehensive gene expression analysis and DNA methylation and hydroxymethylation analysis revealed epigenetic changes in lymphoma cells.

MATERIALS AND METHODS

Mice

Tet2 gene trap mice, in which a poly-A trapping cassette containing the β-galactosidase/neomycin resistance gene is inserted into the second intron,[31] were purchased from TransGenic Inc. (Kumamoto, Japan). Mice were genotyped by tail DNA PCR using the primers listed in Supplementary Table 7. Mice were backcrossed >8 times onto a C57BL/6 background. Experiments were performed according to the Guide for Care and Use of Laboratory Animals at the University of Tsukuba.

[1]Department of Hematology, University of Tsukuba Hospital, Tsukuba, Ibaraki, Japan; [2]Graduate School of Comprehensive Human Science, University of Tsukuba, Tsukuba, Ibaraki, Japan; [3]Faculty of Medicine, Department of Hematology, University of Tsukuba, Tsukuba, Ibaraki, Japan; [4]Genome Science Division, Research Center for Advanced Science and Technology, The University of Tokyo, Meguro-ku, Tokyo, Japan; [5]Department of Pathology and Tumor Biology, Graduate School of Medicine, Kyoto University, Kyoto, Japan; [6]Life Science center, Tsukuba Advanced Research Alliance, University of Tsukuba, Tsukuba, Ibaraki, Japan; [7]Department of Molecular Biological Oncology, Faculty of Medicine, University of Tsukuba, Tsukuba, Ibaraki, Japan; [8]Department of Clinical Laboratory, University of Tsukuba Hospital, Tsukuba, Ibaraki, Japan and [9]Department of Pathology, Tokai University School of Medicine, Isehara, Kanagawa, Japan. Correspondence: Professor S Chiba, Department of Hematology, Faculty of Medicine, University of Tsukuba, 1-1-1 Tennodai, Tsukuba 305-8575, Ibaraki, Japan.
E-mail: schiba-t@md.tsukuba.ac.jp
Received 30 September 2014; accepted 2 October 2014

Gene expression array analysis

Gene expression analysis was carried out with samples from CD4^{+} cells from lymphoma-developing $Tet2^{gt/gt}$ mice or from wild-type (WT) mice with GeneChip Mouse Gene 1.0 ST Array (Affymetrix, Santa Clara, CA, USA), according to the manufacturer's instructions. The Gene Expression Omnibus (GEO) accession number for the microarray data reported in this paper is GSE52430. See Supplementary Methods for more information.

MeDIP and hMeDIP sequencing

MeDIP and hMeDIP sequencing protocols were performed as described, with minor modifications.[32] The DNA Data Bank of Japan (DDBJ) accession numbers are DRA001275 and DRA001277. See Supplementary Methods for more information. See Supplementary information for more methods.

RESULTS

Decreased Tet2 function significantly increases the number of Tfh-like cells in the spleen

We analyzed homozygous Tet2 (hereafter named $Tet2^{gt/gt}$) mice harboring a gene-trap vector in the Tet2 second intron (Supplementary Figure S1a).[31] We reproduced various findings described in previous papers using the same mice, such as 80% decrease in Tet2 mRNA levels and 50% decrease in hmC levels in fetal liver (FL) lineage-negative cells (Supplementary Figures S1b and c), and enhanced repopulating activity in FL LSK cells only after secondary transplantation (Supplementary Figures S2a and b).[29,30] $Tet2^{gt/gt}$ mice were born and grew almost normally at a frequency of a half the expected Mendelian ratio ($Tet2^{gt/gt}$: $Tet2^{+/gt}$:$Tet2^{+/+} = 32$:124:70). There were no significant differences in appearance, complete blood cell counts and proportions of granulocytes, T cells and B cells in the peripheral blood among $Tet2^{gt/gt}$, heterozygous ($Tet2^{+/gt}$) and $Tet2^{+/+}$ mice during the period between 40 and 60 weeks of age (Supplementary Figures S3a and b).

When evaluated at 40-60 weeks old, the spleen weights of $Tet2^{gt/gt}$ mice were significantly higher than those of $Tet2^{+/gt}$ and $Tet2^{+/+}$ mice (179.8 ± 72.3 mg, 97.0 ± 10.6 mg and 108.5 ± 26.1 mg, respectively) (Figure 1a). One of the 10 $Tet2^{gt/gt}$ mice developed marked splenomegaly (> 300 mg). Hematoxylin-Eosin (HE) staining demonstrated preserved follicular structures, having enlarged germinal centers in some $Tet2^{gt/gt}$ mice (Figure 1b).

Next we used flow cytometry to analyze splenocyte phenotypes and observed no differences in proportions of CD4^{+} T cells and B220^{+} B lymphocytes between $Tet2^{gt/gt}$, $Tet2^{+/gt}$ and $Tet2^{+/+}$ mice, although the proportion of CD3^{+} T cells was marginally, but significantly, decreased in $Tet2^{gt/gt}$ mice compared with those of $Tet2^{+/+}$ mice. The population of Gr1^{+}Mac1^{+} granulocytes was slightly, but significantly, increased in $Tet2^{gt/gt}$ mice compared with that of $Tet2^{+/gt}$ and $Tet2^{+/+}$ mice (Figure 1c). The absolute number of cells was increased in all the fractions of $Tet2^{gt/gt}$ mice compared with those of $Tet2^{+/gt}$ and $Tet2^{+/+}$ mice (Figure 1d). Furthermore, we observed significant increases in the ratios of CD4^{+}CD44^{+}PD1^{+} fraction in $Tet2^{gt/gt}$ mice compared with those of $Tet2^{+/gt}$ and $Tet2^{+/+}$ mice (Figures 1e and f). The ratio of CD4^{+}PD1^{+}Cxcr5^{+} fraction was significantly higher in $Tet2^{gt/gt}$ mice than that in $Tet2^{+/+}$ mice (Figure 1f). The absolute numbers of CD4^{+}CD44^{+}PD1^{+} and CD4^{+}PD1^{+}Cxcr5^{+} fractions were significantly increased in $Tet2^{gt/gt}$compared with that in $Tet2^{+/gt}$ and $Tet2^{+/+}$ mice (Figure 1g). PD1 is a co-stimulatory molecule expressed on Tfh cells, which are in fact marked by co-expression of CD4, PD1 and Cxcr5 in mice.[33] In a similar manner to the analysis above, immunofluorescent staining of spleen tissues also indicated an increase of Tfh-like cells in $Tet2^{gt/gt}$ mice (Figure 1h). Overall, our results indicate that reduced Tet2 function causes outgrowth of Tfh-like cells in the spleen at 40–60 weeks old. Extramedullary hematopoiesis in Tet2-knockout/down mice, as described by others,[14,26,27,30] was not apparent in our analysis, although there was a tendency towards increase in erythroid precursor cells and a statistically significant increase in LSK cells in the spleens of $Tet2^{gt/gt}$ mice compared with mice of other genotypes (Supplementary Figure S4a).

$Tet2^{gt/gt}$ mice develop T-cell lymphoma with Tfh-like features

We next analyzed $Tet2^{gt/gt}$ mice older than 60 weeks and found that five in seven mice developed marked splenomegaly, multiple swollen lymph nodes and multiple nodules in the liver and lungs (median age, 67 weeks old) (Figures 2a–c). HE staining showed that follicular structures in spleens of tumor-developing $Tet2^{gt/gt}$ mice were completely destroyed due to the invasion of large pleomorphic cells exhibiting irregular-shaped nuclei (Figure 2c). These findings implied that $Tet2^{gt/gt}$ mice developed lymphoma. We performed immunofluorescent staining to examine the phenotype of the infiltrating cells, demonstrating that most of the cells expressed CD4^{+}, PD1^{+} and Cxcr5^{+} (Figure 2d). To confirm whether the tumors were T-cell lymphoma, we examined the T-cell receptor (TCR) rearrangement pattern using DNA from CD4^{+} T cells in tumor-developing spleens and lymph nodes, and found that the tumor-derived CD4^{+} T cells demonstrated distinct rearrangement patterns in TCR Vβ/Jβ2. Furthermore, tumor-derived CD4^{+} T cells from the spleen and swollen lymph nodes of a mouse showed identical TCR rearrangement patterns (Figure 2e, related to Table 1). Thus, we concluded that $Tet2^{gt/gt}$ mice developed T-cell lymphoma.

Next, we characterized the lymphoma-developing $Tet2^{gt/gt}$ mice. There were no significant differences in white blood cell count and hemoglobin concentration in the peripheral blood of $Tet2^{gt/gt}$, $Tet2^{+/gt}$ and $Tet2^{+/+}$ mice, while platelet count in lymphoma-developing $Tet2^{gt/gt}$ mice was significantly lower than that of $Tet2^{+/+}$ mice (Figure 3a). The spleen weight of lymphoma-developing $Tet2^{gt/gt}$ mice was significantly higher than that of $Tet2^{+/gt}$ and $Tet2^{+/+}$ mice (1466 ± 1086 mg, 139.3 ± 45.0 mg, and 165 ± 83 mg, respectively) (Figure 3b). In the spleens, the CD4^{+} helper T-cell fractions were significantly increased in $Tet2^{gt/gt}$ mice compared with those of $Tet2^{+/gt}$ and $Tet2^{+/+}$ mice (Figure 3c). The B220[+] B-cell fraction was significantly decreased in $Tet2^{gt/gt}$ mice compared with that of $Tet2^{+/+}$ mice. There was no significant difference in Gr1^{+}/Mac1^{+} myeloid cell fraction. The CD4^{+} T cells were mostly positive for CD44 and PD1, and to a lesser extent for Cxcr5 (Figure 3d). The percentage of CD4^{+}PD1^{+}Cxcr5^{+} Tfh-like cell fraction was significantly higher than that of mice with the other genotypes. There were no differences in the erythroid precursor and LSK fraction in the spleens between the aged $Tet2^{+/+}$ and $Tet2^{+/gt}$ mice (Supplementary Figure S4b).

In the clinical setting, AITL patients often show polyclonal hypergammaglobulinemia. Serum immunoglobulin levels in both $Tet2^{+/+}$ mice and $Tet2^{gt/gt}$ mice, however, did not show significant difference (Supplementary Figure S5).

Taken together, these results indicate that $Tet2^{gt/gt}$ mice develop T-cell lymphomas that exhibit features characteristic of Tfh-like cells, but these T-cell lymphomas do not show pathological or clinical findings relevant to human AITL. PTCL-NOS with Tfh-like features[13] might be the closest counterpart.

Lymphoma cells exhibit gene expression profiles similar to those of Tfh cells

Gene-expression profiles of CD4^{+} cells derived from splenic tumors of $Tet2^{gt/gt}$ mice versus CD4^{+} cells from normal WT spleen (hereafter designated lymphoma cells versus control CD4^{+} cells, respectively) were evaluated using the Kyoto Encyclopedia of Genes and Genomes (KEGG) resource[34] and Gene Set Enrichment Analysis (GSEA).[35] When 903 upregulated genes (> 2 folds) and 896 downregulated genes (< 0.5 folds) were searched, the KEGG brought up enriched terms such as 'cytokine-cytokine interaction' and 'hematopietic cell lineage and immune response' (Supplementary Tables S1 and S2).
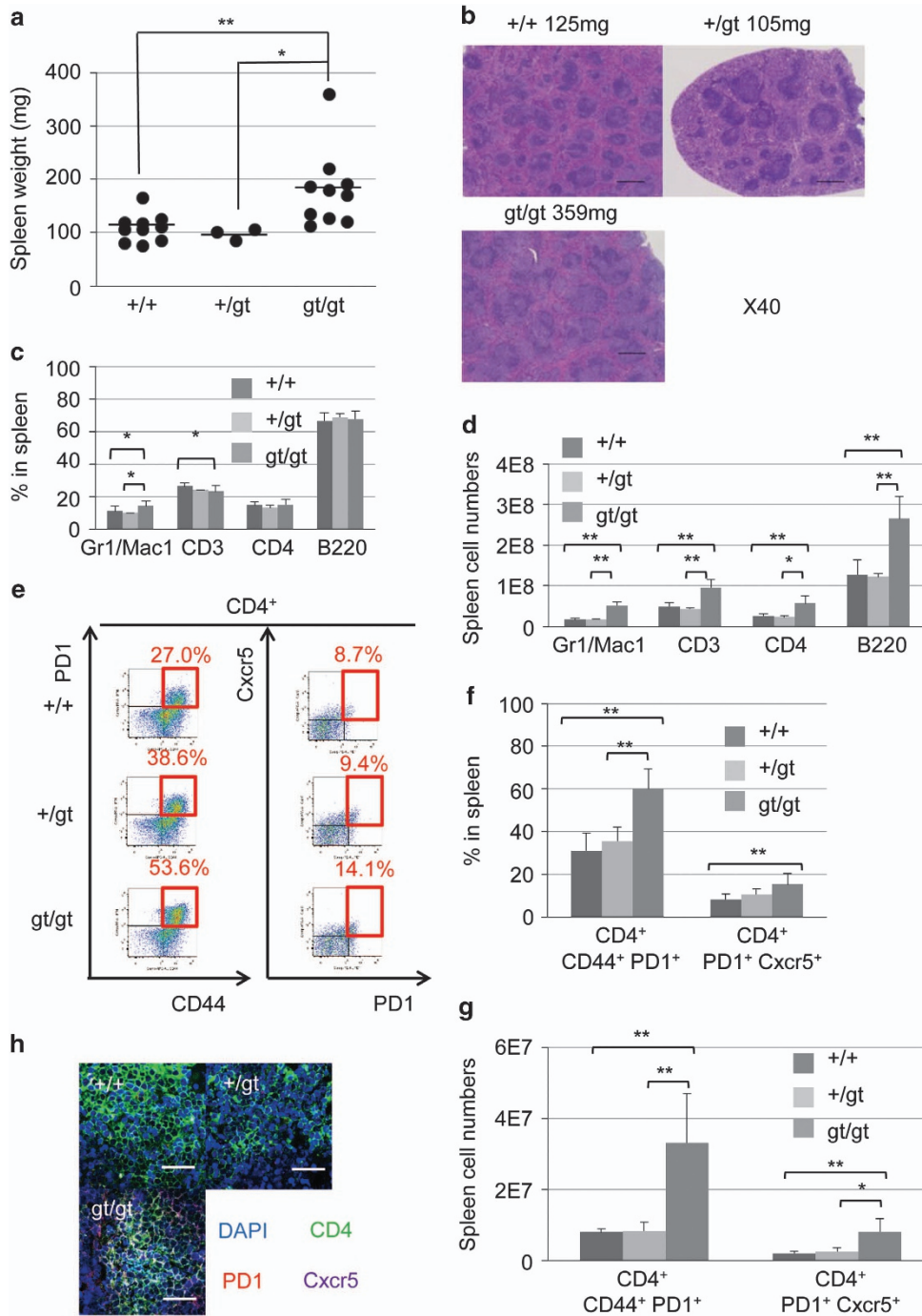
Figure 1. Outgrowth of Tfh-like cells in spleens of 40- to 60-week-old *Tet2$^{gt/gt}$* mice. (**a**) Spleen weights of *Tet2$^{+/+}$*(n = 10), *Tet2$^{+/gt}$* (n = 3) and *Tet2$^{gt/gt}$* (n = 10) mice (mean ± s.d.). *$P < 0.05$, **$P < 0.01$. (**b**) Hematoxylin-Eosin (HE) staining of sections from spleen. Representative figures were shown. Black bars indicate 500 μm. (**c**) Cell surface analysis of splenocytes in *Tet2$^{+/+}$* (n = 10), *Tet2$^{+/gt}$* (n = 3) and *Tet2$^{gt/gt}$*(n = 10) mice (mean ± s.d.). *$P < 0.05$. (**d**) Absolute numbers of splenocytes in each fraction (*Tet2$^{+/+}$* n = 6, *Tet2$^{+/gt}$* n = 3, *Tet2$^{gt/gt}$* n = 6) (mean ± s.d.). *$P < 0.05$, **$P < 0.01$. (**e**) Representative figures of CD4$^+$CD44$^+$PD1$^+$ and CD4$^+$PD1$^+$Cxcr5$^+$ fractions in the spleen of 40- to 60-week-old *Tet2$^{+/+}$*, *Tet2$^{+/gt}$* and *Tet2$^{gt/gt}$* mice. (**f**) Proportions of the CD4$^+$CD44$^+$PD1$^+$ and CD4$^+$PD1$^+$Cxcr5$^+$ fractions in the spleen of *Tet2$^{+/+}$* (n = 9), *Tet2$^{+/gt}$* (n = 3) and *Tet2$^{gt/gt}$* (n = 9) mice (mean ± s.d.). **$P < 0.01$. (**g**) Absolute numbers of CD4$^+$CD44$^+$PD1$^+$ and CD4$^+$PD1$^+$Cxcr5$^+$ cell fractions in the spleen of *Tet2$^{+/+}$* (n = 6), *Tet2$^{+/gt}$* (n = 3) and *Tet2$^{gt/gt}$* (n = 6) mice (mean ± s.d.). *$P < 0.05$, **$P < 0.01$. (**h**) Immunofluorescent staining of 40- to 60-week-old spleen in *Tet2$^{+/+}$*, *Tet2$^{+/gt}$* and *Tet2$^{gt/gt}$*. CD4 (green), PD1 (red) and Cxcr5 (purple) were stained with counter staining of DAPI. White bars indicated 20 μm.

For the GSEA, the Tfh-upregulated gene set was unavailable in BIOCARTA and thus had to be newly made by selecting 21 genes based on previous microarray analyses.[36,37] The Th1/Th2 pathway gene sets were adopted from BIOCARTA for GSEA analysis. The Tfh-upregulated genes were significantly enriched in lymphoma cells compared with control CD4$^+$ cells (P-value 0.0020, FDR Q-value 0.0027, NES 1.869) (Figure 4a). In contrast, genes associated with Th1/2 differentiation were enriched in control CD4$^+$ cells (P-value = 0.0169, FDR Q-value = 0.0169, NES − 1.702) (Figure 4b). To validate the Tfh-like signature in lymphoma cells, we
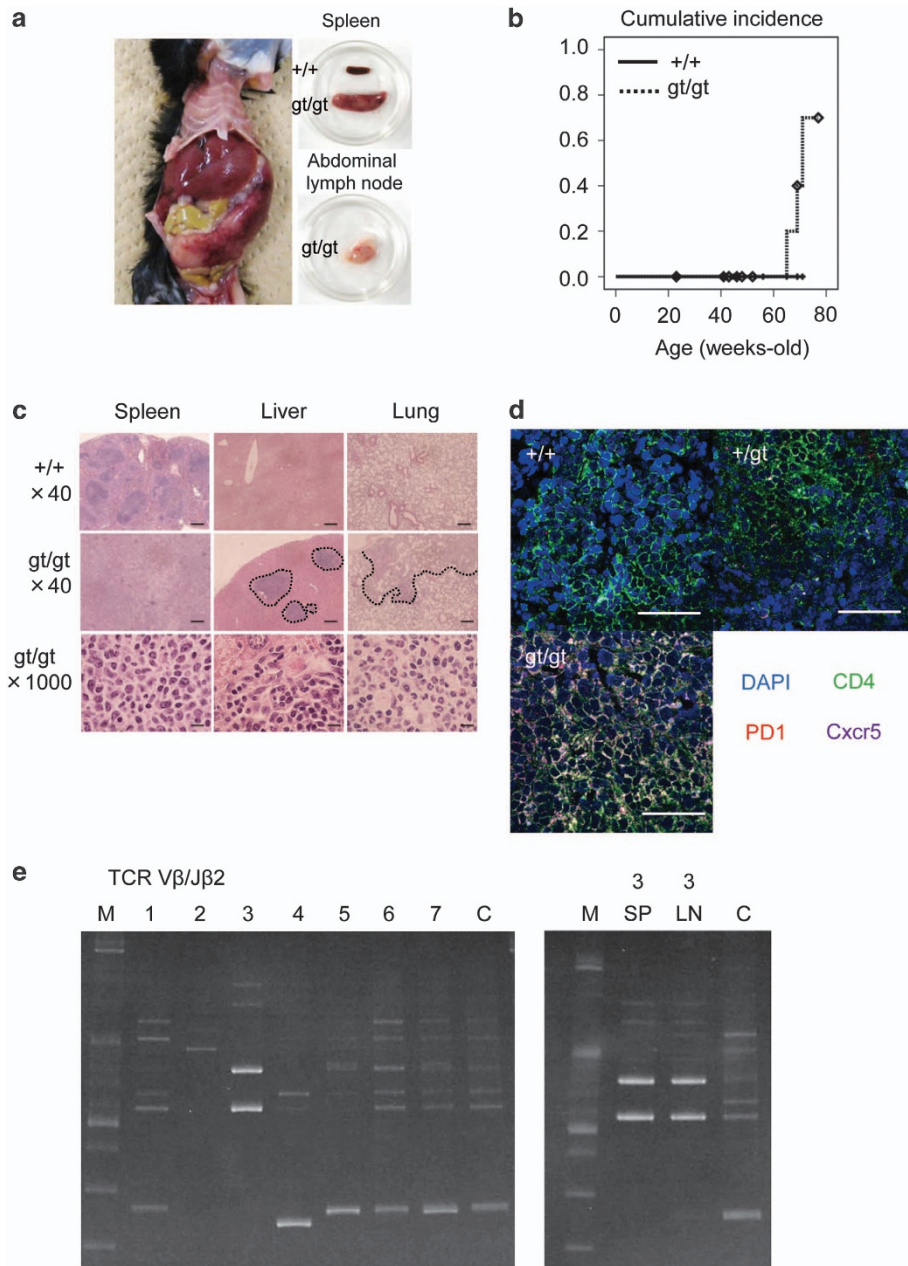
Figure 2. Aged *Tet2^gt/gt* mice develop T-cell lymphoma with Tfh-like features. (**a**) Tumor-developing *Tet2^gt/gt* mouse shows marked splenomegaly (left). Isolated spleen (upper right) and abdominal lymph nodes (lower right) from a *Tet2^+/+* and tumor-developing *Tet2^gt/gt* mouse. (**b**) Cumulative incidence curves of tumor development *in Tet2^+/+* (n = 5) and *Tet2^gt/gt* (n = 7) mice (over 60 weeks old). The median age at onset was 67 weeks old. (**c**) HE staining of sections from the spleen, liver and lung in *Tet2^+/+* (upper) and tumor-developing *Tet2^gt/gt* mice (middle and lower). Dot line indicates lesion of tumor involvements. Black bars in upper and middle panels indicate 200 μm, in lower panels indicate 10 μm. (**d**) Immunofluorescent staining of spleen from aged (>60 weeks) *Tet2^+/+*, aged *Tet2^+/gt* and tumor-developing *Tet2^gt/gt* mice. CD4 (green), PD1 (red) and Cxcr5 (purple) were stained with counter staining of DAPI. White bars indicate 20 μm. (**e**) Analysis of TCRβ rearrangement. Rearrangements of TCR Vβ/Jβ2 are shown. M, marker; C, control; SP, tumor-bearing spleens; LN, swollen lymph node from tumor-developing *Tet2^gt/gt* mice. Numbers indicate individual *Tet2^gt/gt* mice (related to Table 1). Right panel showed TCR rearrangement patterns in the spleen and swollen lymph node of a No.3 *Tet2^gt/gt* mouse.

performed real-time PCR for representative Tfh-associated mRNAs, such as *Bcl6*, *cMaf*, *PD1*, *Icos* and *Cxcr5*. Transcript levels of all these molecules were significantly higher in lymphoma than control CD4^+ cells (Figure 4c). In contrast, transcript levels of *Tbx21* and *Gata3*, which encode master transcription factors regulating Th1 and Th2 differentiation, respectively, were comparable or slightly lower in lymphoma (Figure 4d). In addition, immunofluorescent staining revealed many cells were co-stained for CD4 and Bcl6 or cMaf in lymphoma-developing spleen tissue (Figure 4e).

Lymphoma cells exhibit genome-wide aberrant methylation and hydroxymethylation patterns

To examine potential epigenetic changes in lymphoma cells, we performed methylated DNA immunoprecipitation (MeDIP) and hydroxymethylated DNA immunoprecipitation (hMeDIP) combined with high-throughput sequencing, using three independent samples for lymphoma and control CD4^+ cells. In the gene-oriented analysis, the average level of mC showed a similar pattern in the lymphoma cells and control CD4^+ cells, while the

Table 1. Characteristics of aged $Tet2^{gt/gt}$ mice ($n = 7$ more than 60 weeks old)

No	1	2	3	4	5	6	7
Spleen weight (mg)	433	1615	1437	656	3189	136	167
Macroscopic lymphoma involvement	+	+	+	+	+	−	−
Microscopic lymphoma involvement	+	+	+	+	+	−	−
TCRβ rearrangement	+	+	+	+	+	−	−

Lymphoma involvement includes swollen lymph nodes or organ lesion such as the liver or lung.

hmC level was slightly reduced in lymphoma cells. Focused around the TSS, the average mC level showed a slight decrease just downstream of the TSS, but an increase toward its gene body region in lymphoma cells. In comparison, the decrease of average hmC level was remarkable between TSS and at 5 k bp downstream of TSS in lymphoma cells (Figure 5a). We then examined the distribution of the highly enriched regions of mC and hmC. The regions in which the Model-based analysis for ChIP-Seq (MACS) score was > 5 were considered to be highly enriched regions.[38] Within these regions, methylation at the TSS regions (TSS ± 1 k bp, TSS ± 5 k bp), gene bodies and CpG islands was increased in lymphoma cells in comparison with the control $CD4^+$ cells ($P = 0.013$, 0.006, 0.006 and 0.022, respectively). Hydroxymethylation was decreased at the TSS regions in lymphoma cells
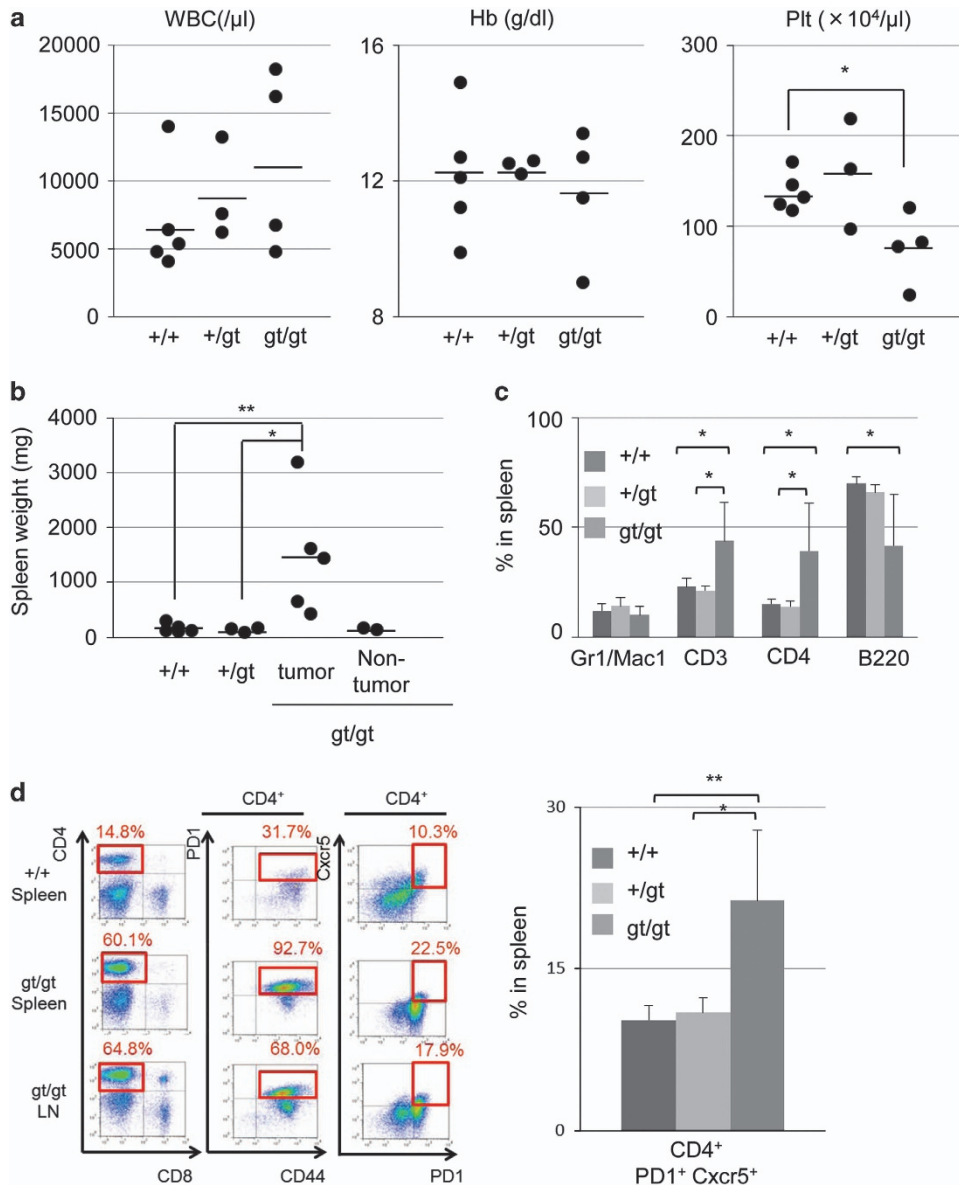

Figure 3. Characteristics of lymphoma-developing $Tet2^{gt/gt}$ mice. (**a**) White blood cell (WBC) counts, hemoglobin (Hb) concentrations and platelet (Plt) counts in aged $Tet2^{+/+}$ ($n = 5$), aged $Tet2^{+/gt}$ ($n = 3$) and lymphoma-developing $Tet2^{gt/gt}$ ($n = 4$) mice over 60 weeks of age. Black bars indicate mean values. *$P < 0.05$. (**b**) Spleen weights of $Tet2^{+/+}$ ($n = 5$), $Tet2^{+/gt}$ ($n = 3$) and lymphoma-developing $Tet2^{gt/gt}$ ($n = 5$) and non-lymphoma-developing $Tet2^{gt/gt}$ mice ($n = 2$). Black bars indicate mean values. *$P < 0.05$, **$P < 0.01$. (**c**) Cell surface analysis of splenocytes in $Tet2^{+/+}$ ($n = 5$), $Tet2^{+/gt}$ ($n = 3$) and lymphoma-developing $Tet2^{gt/gt}$ ($n = 4$) mice (mean ± s.d.). *$P < 0.05$. (**d**) Representative figures of cell surface analyses of the spleen from $Tet2^{+/+}$ mice (upper), and spleen and lymph node (LN) from lymphoma-developing $Tet2^{gt/gt}$ mice (middle and lower) over 60 weeks old. The graph shows the percentages of Tfh-like fractions ($Tet2^{+/+}$ $n = 5$, $Tet2^{+/gt}$ $n = 3$ and $Tet2^{gt/gt}$ $n = 4$; mean ± s.d.). *$P < 0.05$, **$P < 0.01$.

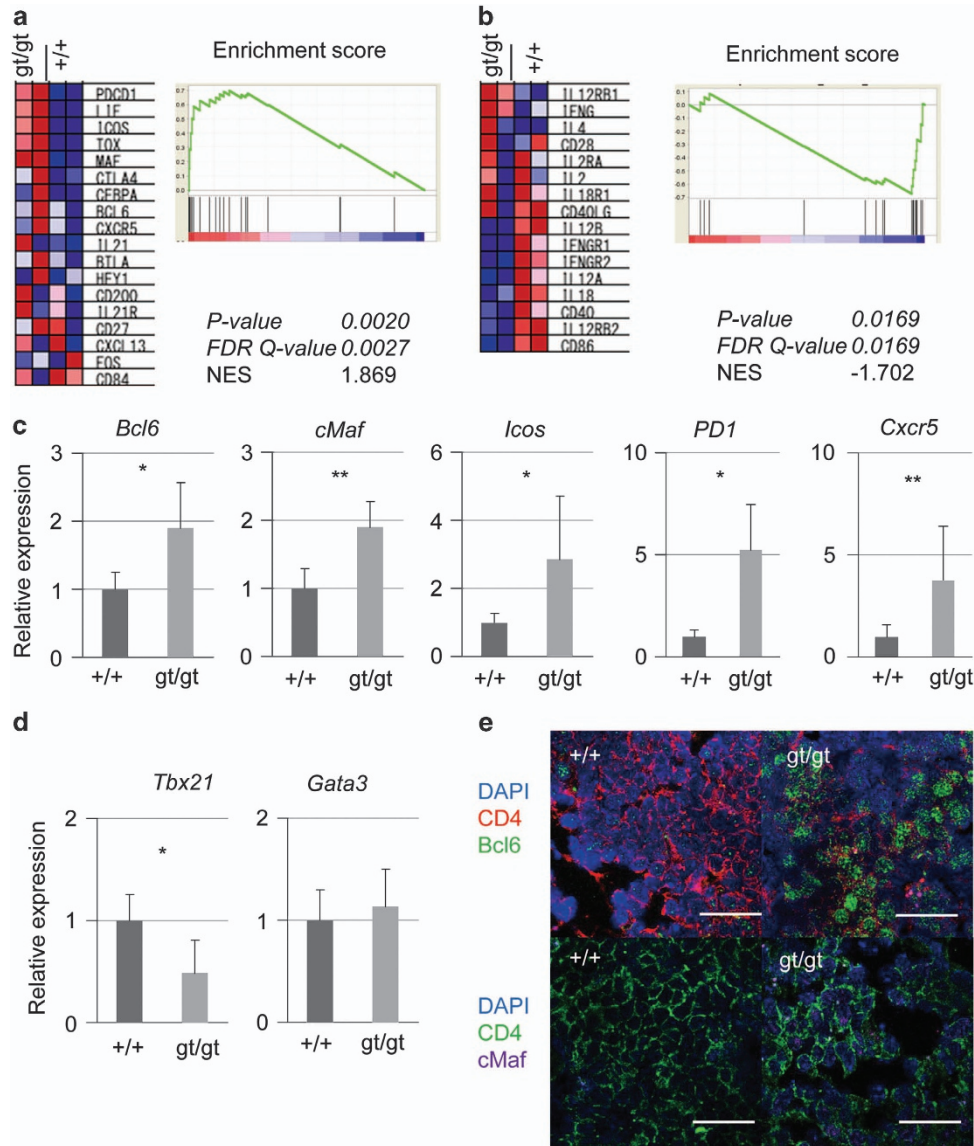**Figure 4.** Tfh-like gene expression patterns in lymphoma cells. (**a**) GSEA analysis of CD4+ cells from spleens of Tet2+/+ (n = 2) compared with lymphoma-developing Tet2gt/gt (n = 2) mice, showing a gene set associated with 21 Tfh-upregulated genes. NES means normalized enrichment score. (**b**) GSEA analysis comparing CD4+ cells from Tet2+/+ (n = 2) and lymphoma-developing Tet2gt/gt (n = 2) mice applying gene set from the Th1 and Th2 pathways. (**c**) mRNA expression as determined by real-time PCR analysis of CD4+ cells from Tet2+/+ (n = 6) and those from lymphoma-developing Tet2gt/gt (n = 5) mice (mean ± s.d.). *P < 0.05, **P < 0.01. (**d**) Real-time PCR analysis of Tbx21 and Gata3 transcripts in CD4+ cells from Tet2+/+(n = 6) and lymphoma-developing Tet2gt/gt (n = 5) mice (mean ± s.d.). *P < 0.05. (**e**) Immunofluorescent staining of Bcl6 (upper) and cMaf (lower) in lymphoma-developing and aged WT spleens. In upper panels, CD4 (red) and Bcl6 (green) with counter staining of DAPI. In lower panels, CD4 (green) and cMaf (purple) with counter staining of DAPI. White bars indicated 30 µm.

compared with the control CD4+ cells (P = 0.018 and 0.006, respectively) (Figure 5b).

Next, we merged the two gene lists, the first for upregulated gene expression and the second for aberrant deposition of methylation or hydroxymethylation. Generally, DNA methylation in the promoter region is closely associated with the inactivation of gene expression. In contrast, aberrant accumulation of methylation in the gene body is known to be associated with upregulated transcription.[39] The tumor cells in our T-cell lymphoma mouse model showed Tfh-like cell outgrowth and lymphoma cells showed upregulation in the Tfh-related genes. Thus, we selected 2555 genes (upper 10% of total genes) showing greater mC density at the gene body regions in lymphoma cells compared with the control CD4+ cells (mean difference of tag

counts by MACS > 7). Independently, we selected 2500 highly expressed genes (upper 10% of total genes), and the top 903 genes with an expression fold of > 2 in lymphoma cells compared with control CD4+ cells. In these two groups, 448 and 118 genes, respectively, fulfilled both criteria of mC increase in gene body and fold change in gene expression. Gene ontology (GO) analysis picked up several enriched terms associated with oncogenesis, such as regulation of cell death and anti-apoptosis for the 448 genes (Supplementary Table S3), and cell division, cell cycle and cell cycle process (Supplementary Table S4) for the 118 genes (Figure 5c).

We similarly selected 2639 genes (upper 10% of total genes) (mean difference of tag counts by MACS < − 3) showing lower hmC density at the TSS ± 1 k bp regions in lymphoma cells
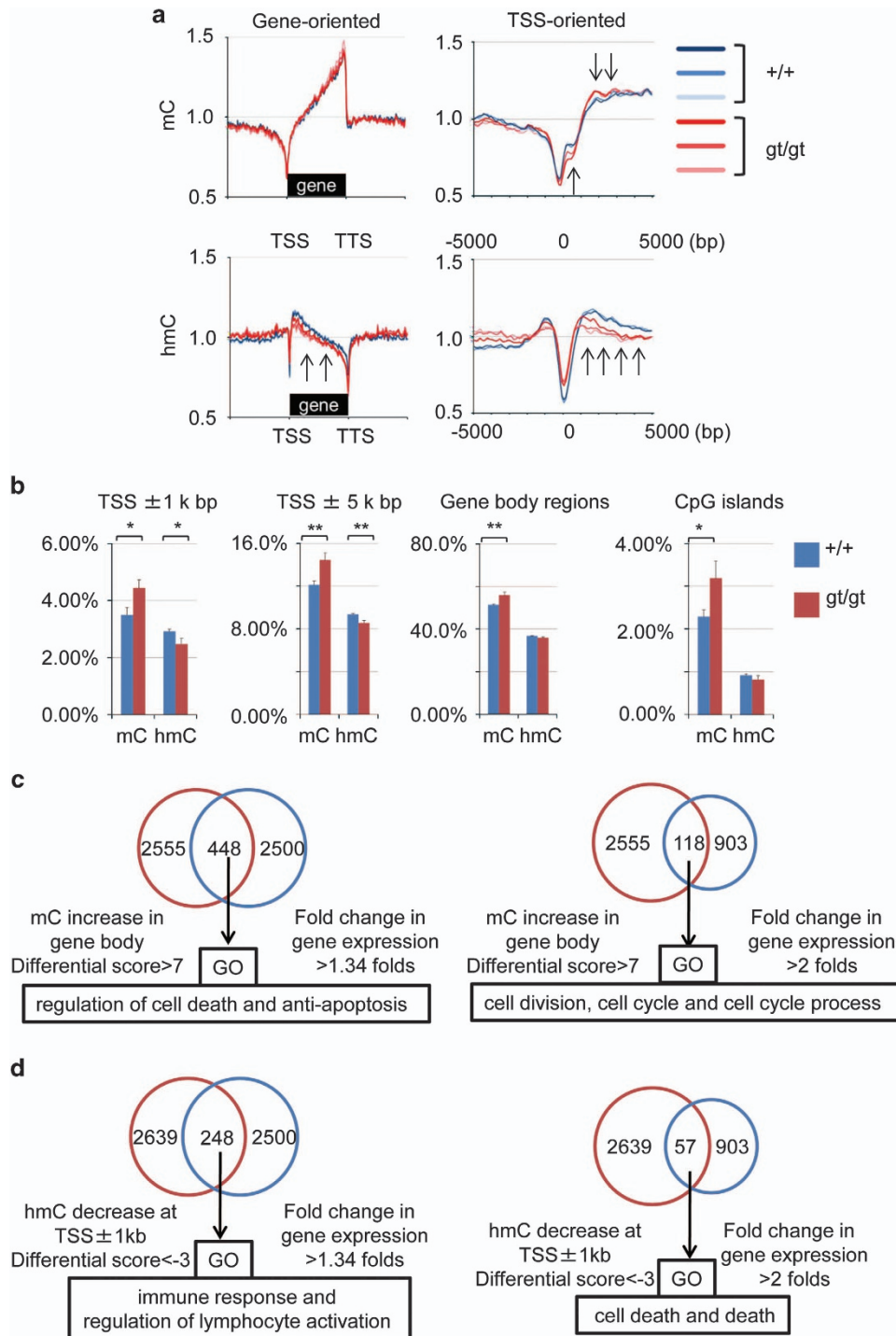
Figure 5. Genome-wide mC and hmC analysis of CD4$^+$ spleen cells from Tet2$^{+/+}$ and lymphoma-developing Tet2$^{gt/gt}$ mice. (**a**) Average levels of mC (upper) and hmC (lower) in CD4$^+$ splenocytes from Tet2$^{+/+}$ ($n=3$) and lymphoma-developing Tet2$^{gt/gt}$ ($n=3$) mice. Left graphs indicate gene-oriented distribution of mC and hmC; right graphs indicate mC and hmC distribution around the transcription start site (TSS). TTS, transcription termination site. Black allows indicate the regions at differences between lymphoma cells and control cells. (**b**) Distribution of mC and hmC enriched regions (MACS score >5) at TSS±1 k bp, TSS±5 k bp, gene body regions and CpG islands in CD4$^+$ splenocytes from Tet2$^{+/+}$ ($n=3$) and lymphoma-developing Tet2$^{gt/gt}$ ($n=3$) mice. (**c**) The top 2555 genes showing increased methylation at the gene body in lymphoma cells compared with control CD4$^+$ cells were selected, as were the top 2500 and 903 genes showing higher expression in lymphoma compared with control CD4$^+$ cells; 448 and 118 genes were common to both groups, respectively. Gene ontology (GO) analysis was performed using these genes. Each term was shown. (**d**) The top 2639 genes showing decreased hydroxymethylation in the gene body in lymphoma cells compared with control CD4$^+$ cells were selected, as were the top 2500 and 903 genes showing higher expression in lymphoma compared with control CD4$^+$ cells. 248 and 57 genes were common to both groups, respectively. GO analysis was performed using these genes.
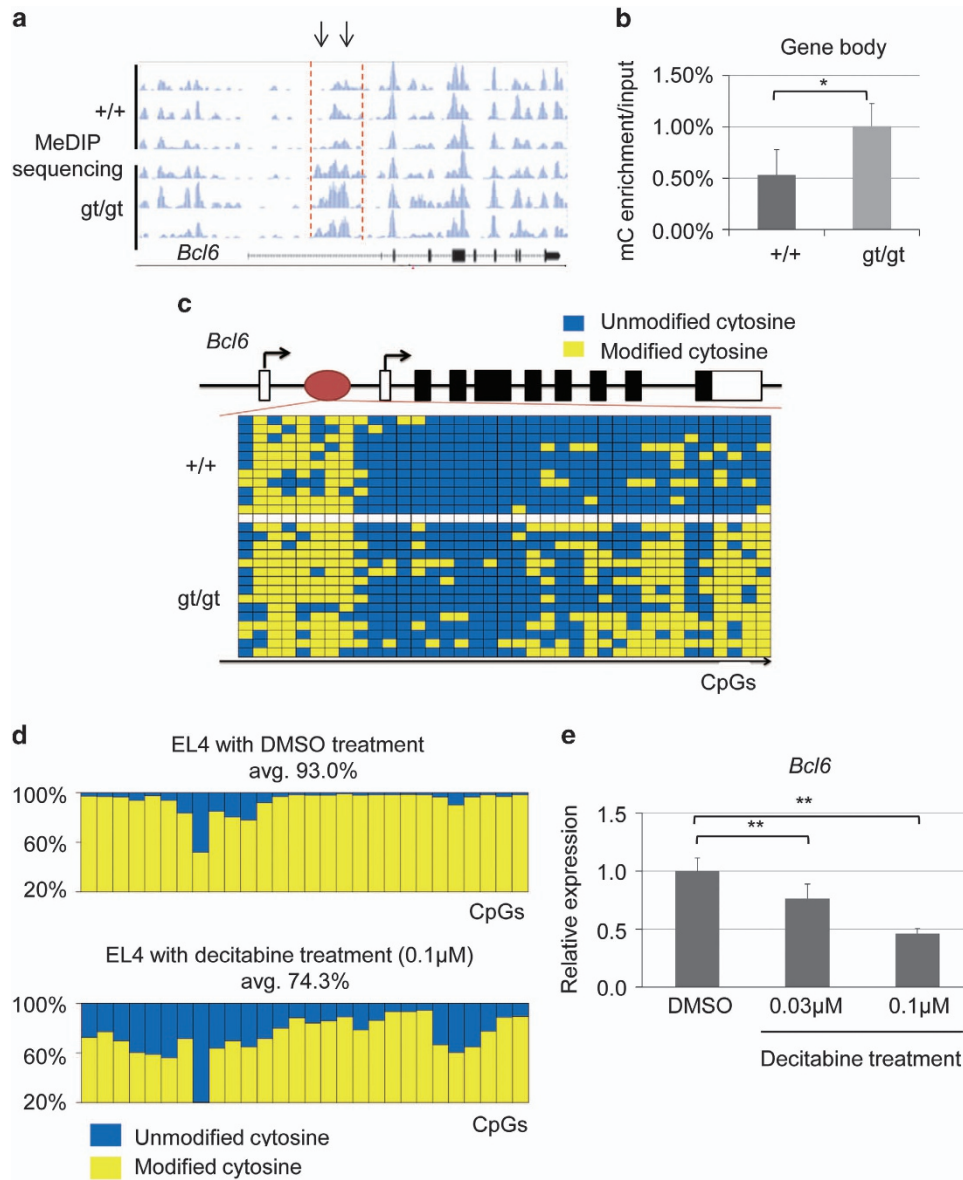
Figure 6. Methylation status at *Bcl6* in *Tet2*^{+/+} mice and lymphoma-developing *Tet2*[gt/gt] mice and those in EL4 cells with decitabine treatment. (**a**) Results of MeDIP sequencing of the *Bcl6* locus in CD4^{+} cells from *Tet2*^{+/+} (n = 3) and lymphoma-developing *Tet2*[gt/gt] (n = 3) mice. The *Bcl6* first intron was hypermethylated in lymphoma cells (area between red dashed lines with black allows). (**b**) Quantitative MeDIP analysis at the first intron of *Bcl6* in CD4^{+} cells from *Tet2*^{+/+} (n = 4) and lymphoma-developing *Tet2*[gt/gt] (n = 3) mice (mean ± s.d.). mC level in *Tet2*[gt/gt] mice was significantly increased at this region compared with that in *Tet2*^{+/+} mice. *$P < 0.05$. (**c**) Bisulfite sequencing at the first intron of *Bcl6* locus in CD4^{+} cells from *Tet2*^{+/+}and lymphoma-developing *Tet2*[gt/gt] mice. Representative data from two independent experiments are shown. (**d**) Bisulfite sequencing of the *Bcl6* int1-S in EL4 mouse T-cell lymphoma cells treated with or without decitabine (n = 3). Representative data from two independent experiments are shown. (**e**) *Bcl6* mRNA levels in EL4 cells treated with or without decitabine based on real-time PCR analysis (n = 3) (mean ± s.d.). Representative data from three independent experiments are shown. **$P < 0.01$.

compared with the control CD4^{+} cells, in light of a recent report demonstrating that hmC at the promoter region negatively regulates gene expression.[40] When the same 2500 and 903 highly expressed genes were analyzed, 248 and 57 genes, respectively, fulfilled both criteria of hmC increase at TSS − 1 k bp and fold change in gene expression (Figure 5d). GO analysis picked up enriched terms such as immune response and regulation of lymphocyte activation (Supplementary Table S5), and cell death and death (Supplementary Table S6) for the 248 and 57 genes, respectively.

These analyses suggest that the gene list overlapping highly methylated genes at the gene body and upregulated genes in

lymphoma cells is linked to oncogenesis, and that the gene list overlapping less hydroxymethylated genes at TSS and upregulated genes in lymphoma cells is linked to the immune system.

Bcl6 was one of the 448 genes associated with mC change that arose in our analyses of the Tfh-related genes enriched in lymphoma cells. MeDIP sequencing of the *Bcl6* locus revealed a markedly increased mC density in the first intron in lymphoma compared with the control CD4^{+} cells (Figure 6a). The change in the mC density in the first intron was validated by quantitative MeDIP (qMeDIP) (Figure 6b). hmC analysis as described above revealed *PD1* and *Cxcr5* to be among the Tfh-related genes. hmC peaks were decreased in TSS ± 1 k bp of *PD1* and *Cxcr5* genes

Table 2.	Validated gene list of exome sequencing with paired-normal control (No.5)				
Annotated gene	Mutation type	Ref Seq	Nucleotide change	Amino-acid change	VAF
Cadm2	Missense	NM_001145977	c.A512T	p.Y171F	0.133333
Angel2	Missense	NM_021421	c.G1349A	p.S450N	0.178571
Skint10	Missense	NM_177668	c.C395A	p.T132N	0.147059
Taar5	Missense	NM_001009574	c.G880C	p.A294P	0.150327
Bcl6	Missense	NM_009744	c.G1049A	p.S350N	0.179487

Abbreviation: VAF, valiant allele frequency.

(Supplementary Figures S6a and S6c). Quantitative hMeDIP also showed tendencies of hmC decrease in TSS ± 1 k bp of both genes, but there was no statistical significance (Supplementary Figure S6b and S6d).

These results prompted us to further analyze the first intron of the Bcl6 gene, which has been reported as an intronic silencer region (Bcl6 int1-S), the silencing activity of which depends on its methylation status in a human B-cell lymphoma cell line.[41] BCL6 plays a definitive role for the development of Tfh cells.[20] Bisulfite sequencing revealed an increase in the density of modified cytosine at the first intron in lymphoma relative to control cells (Figure 6c), corresponding to the MeDIP sequencing (Figure 6a).

Decitabine-induced demethylation of the first intron of Bcl6 decreases mRNA expression in EL4 cells

To determine whether methylation-dependent regulation of Bcl6 expression occurs in T-lineage lymphoma cells, we examined Bcl6 mRNA expression and methylation status in EL4 cells, a mouse T-cell lymphoma cell line. Bisulfite sequencing revealed that almost all cytosines found in CpG sequences were methylated at the Bcl6 int1-S in EL4 cells. Following treatment of EL4 cells with the demethylating agent decitabine, levels of the methylated cytosines decreased (Figure 6d). Accordingly, Bcl6 transcript levels decreased in a decitabine dose-dependent manner (Figure 6e). This result supports the notion that the methylated cytosine density at the Bcl6 int1-S positively regulates Bcl6 transcription in T cells.

Frequently coexisting mutations with TET2 mutation in hematologic malignancies are not detected by exome and targeted sequencing

To examine additional mutations in lymphoma cells, we performed exome sequencing in the lymphoma cells developed in Tet2$^{gt/gt}$ mice (sample No.5 in Table 1). Five gene mutations were identified and validated by Sanger sequencing, but none of these mutations have been reported in connection with human peripheral T-cell lymphoma (Table 2).[12,42,43] In contrast, Flt3, Npm1, Dnmt3a, Idh2 and Rhoa mutations, which are known to coexist with TET2 mutations in various human hematologic malignancies, were not identified by targeted sequencing in tumor sample numbers 1 to 5 (Supplementary Figure S7).

DISCUSSION

Here, we report a new mouse model of T-cell lymphoma with Tfh-like features and a long latency following proliferation of non-neoplastic Tfh-like CD4$^+$ T cells. Reduced Tet2 function possibly contributes to perturbed conversion of mC to hmC, an essential intermediary in the demethylation process. Genome-wide methylation analysis of lymphoma cells revealed an abnormal accumulation of mC. Further analysis suggested that one of the important targets for Tfh-like cell outgrowth might be an increase of methylation level at Bcl6 int1-S.

Heterozygous mutations in the Roquin gene, which encodes a protein that binds to and reduces the stability of Icos mRNA, also promotes T-cell lymphoma accompanied by Tfh features in mice. Roquin mutations, however, have not been identified in human AITL samples.[12,44–46] Given this, our mouse model recapitulates human T-lymphomagenesis more closely than the Roquin model. Nevertheless, other characteristics of human AITL, such as polyclonal hypergammaglobulinemia, proliferation of high endothelial venules, and infiltration of eosinophils and B cells, were not seen. Our model mimics PTCL-NOS with Tfh-like features in humans.

Bcl6 has been reported to direct Tfh-cell differentiation.[20] Bcl6-deficient T cells fail to develop into Tfh cells and cannot sustain germinal center responses, whereas forced expression of Bcl6 in CD4$^+$ T cells promotes expression of Cxcr5 and PD1, which encodes Tfh-cell markers. Furthermore, transgenic mice constitutively expressing Bcl6 protein in lymphocytes develop B- and T-cell lymphomas. In this model, lymphoma development required a long latency period, and the incidence was markedly enhanced by administration of N-ethyl-N-nitrosourea (ENU), which is known to induce DNA mutations.[47] In this paper we have shown that Tet2$^{gt/gt}$ mice develop lymphoma with a long latency, similar to Bcl6 transgenic mice. Thus, impaired Tet2 or enhanced Bcl6 in isolation might induce a premalignant state, but be insufficient to induce lymphoma development in mice. Given that TET2 somatic mutations occur in 5.6% of elderly females with skewed X-inactivation without hematological malignancies,[48] additional mutations may be required for lymphoma development. We recently reported that 38 out of 46 (82.6%) clinical AITL samples had mutations in TET2 throughout the coding region, and that 32 out of the 46 (69.5%) samples had mutations in both TET2 and ras homology family A (RHOA).[12] The RHOA mutations were accumulated in amino-acid position 17. Other groups also reported the high frequency of RHOA mutations in AITL patients.[42,43] In our mouse lymphoma samples, however, the G17 RHOA mutation was not detected, as well as any other frequently coexisting mutations with TET2 mutations in human hematological malignancies. Genomic evolution of T-cell lymphoma in our mouse model was different from that in humans.

DNA derived from AML samples harboring mutations in IDH1/2, which regulates TET2 function, is hypermethylated.[10] DNA from diffuse large B-cell lymphoma samples harboring TET2 mutations also shows hypermethylation.[49] In contrast, hydroxymethylation status has not been widely assessed in any hematologic malignancies. It is known that hmC is particularly enriched at TSS regions of genes in ES cells,[50] suggesting that hmC functions in transcriptional regulation. The marked hmC reduction at TSS regions of lymphoma cells reported here suggests that impaired TET2 function might alter transcription via reduction in the hmC epigenetic mark, in addition to impaired demethylation.

In summary, we conclude that Tet2$^{gt/gt}$ mice develop T-cell lymphoma with Tfh-like features with epigenetic changes. Hypermethylation of Bcl6 int1-S possibly contributes to the upregulation of Bcl6 and outgrowth of Tfh-like cells. Demethylating agents, such as azacitidine and decitabine, are reportedly effective for treating MDS.[51,52] These agents may also possibly target T-cell lymphomas, particularly those that harbor mutations in epigenetic regulators.

CONFLICT OF INTEREST

The authors declare no conflict of interest.

REFERENCES

1 Tahiliani M, Koh KP, Shen Y, Pastor WA, Bandukwala H, Brudno Y et al. Conversion of 5-methylcytosine to 5-hydroxymethylcytosine in mammalian DNA by MLL partner TET1. Science 2009; 324: 930–935.

2 Ito S, D'Alessio AC, Taranova OV, Hong K, Sowers LC, Zhang Y. Role of Tet proteins in 5mC to 5hmC conversion, ES-cell self-renewal and inner cell mass specification. Nature 2010; 466: 1129–1133.

3 Branco MR, Ficz G, Reik W. Uncovering the role of 5-hydroxymethylcytosine in the epigenome. Nat Rev Genet 2011; 13: 7–13.

4 Ko M, Huang Y, Jankowska AM, Pape UJ, Tahiliani M, Bandukwala HS et al. Impaired hydroxylation of 5-methylcytosine in myeloid cancers with mutant TET2. Nature 2010; 468: 839–843.

5 Kriukiene E, Liutkeviciute Z, Klimasauskas S. 5-Hydroxymethylcytosine–the elusive epigenetic mark in mammalian DNA. Chem Soc Rev 2012; 41: 6916–6930.

6 Abdel-Wahab O, Mullally A, Hedvat C, Garcia-Manero G, Patel J, Wadleigh M et al. Genetic characterization of TET1, TET2, and TET3 alterations in myeloid malignancies. Blood 2009; 114: 144–147.

7 Delhommeau F, Dupont S, Della Valle V, James C, Trannoy S, Masse A et al. Mutation in TET2 in myeloid cancers. N Engl J Med 2009; 360: 2289–2301.

8 Langemeijer SM, Kuiper RP, Berends M, Knops R, Aslanyan MG, Massop M et al. Acquired mutations in TET2 are common in myelodysplastic syndromes. Nat Genet 2009; 41: 838–842.

9 Jankowska AM, Szpurka H, Tiu RV, Makishima H, Afable M, Huh J et al. Loss of heterozygosity 4q24 and TET2 mutations associated with myelodysplastic/myeloproliferative neoplasms. Blood 2009; 113: 6403–6410.

10 Figueroa ME, Abdel-Wahab O, Lu C, Ward PS, Patel J, Shih A et al. Leukemic IDH1 and IDH2 mutations result in a hypermethylation phenotype, disrupt TET2 function, and impair hematopoietic differentiation. Cancer Cell 2010; 18: 553–567.

11 Perez C, Martinez-Calle N, Martin-Subero JI, Segura V, Delabesse E, Fernandez-Mercado M et al. TET2 mutations are associated with specific 5-methylcytosine and 5-hydroxymethylcytosine profiles in patients with chronic myelomonocytic leukemia. PLoS One 2012; 7: e31605.

12 Sakata-Yanagimoto M, Enami T, Yoshida K, Shiraishi Y, Ishii R, Miyake Y et al. Somatic RHOA mutation in angioimmunoblastic T cell lymphoma. Nat Genet 2014; 46: 171–175.

13 Lemonnier F, Couronne L, Parrens M, Jais JP, Travert M, Lamant L et al. Recurrent TET2 mutations in peripheral T-cell lymphomas correlate with TFH-like features and adverse clinical parameters. Blood 2012; 120: 1466–1469.

14 Quivoron C, Couronne L, Della Valle V, Lopez CK, Plo I, Wagner-Ballon O et al. TET2 inactivation results in pleiotropic hematopoietic abnormalities in mouse and is a recurrent event during human lymphomagenesis. Cancer Cell 2011; 20: 25–38.

15 de Leval L, Gisselbrecht C, Gaulard P. Advances in the understanding and management of angioimmunoblastic T-cell lymphoma. Br J Haematol 2010; 148: 673–689.

16 de Leval L, Rickman DS, Thielen C, Reynies A, Huang YL, Delsol G et al. The gene expression profile of nodal peripheral T-cell lymphoma demonstrates a molecular link between angioimmunoblastic T-cell lymphoma (AITL) and follicular helper T (TFH) cells. Blood 2007; 109: 4952–4963.

17 Vinuesa CG, Tangye SG, Moser B, Mackay CR. Follicular B helper T cells in antibody responses and autoimmunity. Nat Rev Immunol 2005; 5: 853–865.

18 Fazilleau N, Mark L, McHeyzer-Williams LJ, McHeyzer-Williams MG. Follicular helper T cells: lineage and location. Immunity 2009; 30: 324–335.

19 Kroenke MA, Eto D, Locci M, Cho M, Davidson T, Haddad EK et al. Bcl6 and Maf cooperate to instruct human follicular helper CD4 T cell differentiation. J Immunol 2012; 188: 3734–3744.

20 Yu D, Rao S, Tsai LM, Lee SK, He Y, Sutcliffe EL et al. The transcriptional repressor Bcl-6 directs T follicular helper cell lineage commitment. Immunity 2009; 31: 457–468.

21 Nurieva RI, Chung Y, Martinez GJ, Yang XO, Tanaka S, Matskevitch TD et al. Bcl6 mediates the development of T follicular helper cells. Science 2009; 325: 1001–1005.

22 Ree HJ, Kadin ME, Kikuchi M, Ko YH, Suzumiya J, Go JH. Bcl-6 expression in reactive follicular hyperplasia, follicular lymphoma, and angioimmunoblastic T-cell lymphoma with hyperplastic germinal centers: heterogeneity of intrafollicular T-cells and their altered distribution in the pathogenesis of angioimmunoblastic T-cell lymphoma. Hum Pathol 1999; 30: 403–411.

23 Natkunam Y, Tedoldi S, Paterson JC, Zhao S, Rodriguez-Justo M, Beck AH et al. Characterization of c-Maf transcription factor in normal and neoplastic hematolymphoid tissue and its relevance in plasma cell neoplasia. Am J Clin Pathol 2009; 132: 361–371.

24 Hiramatsu Y, Suto A, Kashiwakuma D, Kanari H, Kagami S, Ikeda K et al. c-Maf activates the promoter and enhancer of the IL-21 gene, and TGF-beta inhibits c-Maf-induced IL-21 production in CD4+ T cells. J Leukoc Biol 2010; 87: 703–712.

25 Chen M, Guo Z, Ju W, Ryffel B, He X, Zheng SG. The development and function of follicular helper T cells in immune responses. Cell Mol Immunol 2012; 9: 375–379.

26 Moran-Crusio K, Reavie L, Shih A, Abdel-Wahab O, Ndiaye-Lobry D, Lobry C et al. Tet2 loss leads to increased hematopoietic stem cell self-renewal and myeloid transformation. Cancer Cell 2011; 20: 11–24.

27 Li Z, Cai X, Cai CL, Wang J, Zhang W, Petersen BE et al. Deletion of Tet2 in mice leads to dysregulated hematopoietic stem cells and subsequent development of myeloid malignancies. Blood 2011; 118: 4509–4518.

28 Ko M, Bandukwala HS, An J, Lamperti ED, Thompson EC, Hastie R et al. Ten-Eleven-Translocation 2 (TET2) negatively regulates homeostasis and differentiation of hematopoietic stem cells in mice. Proc Natl Acad Sci USA 2011; 108: 14566–14571.

29 Kunimoto H, Fukuchi Y, Sakurai M, Sadahira K, Ikeda Y, Okamoto S et al. Tet2 disruption leads to enhanced self-renewal and altered differentiation of fetal liver hematopoietic stem cells. Sci Rep 2012; 2: 273.

30 Shide K, Kameda T, Shimoda H, Yamaji T, Abe H, Kamiunten A et al. TET2 is essential for survival and hematopoietic stem cell homeostasis. Leukemia 2012; 26: 2216–2223.

31 Tang H, Araki K, Li Z, Yamamura K. Characterization of Ayu17-449 gene expression and resultant kidney pathology in a knockout mouse model. Transgenic Res 2008; 17: 599–608.

32 Ficz G, Branco MR, Seisenberger S, Santos F, Krueger F, Hore TA et al. Dynamic regulation of 5-hydroxymethylcytosine in mouse ES cells and during differentiation. Nature 2011; 473: 398–402.

33 Gaulard P, de Leval L. Follicular helper T cells: implications in neoplastic hematopathology. Semin Diagn Pathol 2011; 28: 202–213.

34 Ogata H, Goto S, Fujibuchi W, Kanehisa M. Computation with the KEGG pathway database. Biosystems 1998; 47: 119–128.

35 Subramanian A, Tamayo P, Mootha VK, Mukherjee S, Ebert BL, Gillette MA et al. Gene set enrichment analysis: a knowledge-based approach for interpreting genome-wide expression profiles. Proc Natl Acad Sci USA 2005; 102(43): 15545–15550.

36 Chtanova T, Tangye SG, Newton R, Frank N, Hodge MR, Rolph MS et al. T follicular helper cells express a distinctive transcriptional profile, reflecting their role as non-Th1/Th2 effector cells that provide help for B cells. J Immunol 2004; 173: 68–78.

37 Chtanova T, Newton R, Liu SM, Weininger L, Young TR, Silva DG et al. Identification of T cell-restricted genes, and signatures for different T cell responses, using a comprehensive collection of microarray datasets. J Immunol 2005; 175: 7837–7847.

38 Zhang Y, Liu T, Meyer CA, Eeckhoute J, Johnson DS, Bernstein BE et al. Model-based analysis of ChIP-Seq (MACS). Genome Biol 2008; 9: R137.

39 Jones PA. Functions of DNA methylation: islands, start sites, gene bodies and beyond. Nat Rev Genet 2012; 13(7): 484–492.

40 Robertson J, Robertson AB, Klungland A. The presence of 5-hydroxymethylcytosine at the gene promoter and not in the gene body negatively regulates gene expression. Biochem Biophys Res Commun 2011; 411: 40–43.

41 Lai AY, Fatemi M, Dhasarathy A, Malone C, Sobol SE, Geigerman C et al. DNA methylation prevents CTCF-mediated silencing of the oncogene BCL6 in B cell lymphomas. J Exp Med 2010; 207: 1939–1950.

42 Palomero T, Couronne L, Khiabanian H, Kim MY, Ambesi-Impiombato A, Perez-Garcia A et al. Recurrent mutations in epigenetic regulators, RHOA and FYN kinase in peripheral T cell lymphomas. Nat Genet 2014; 46: 166–170.

43 Yoo HY, Sung MK, Lee SH, Kim S, Lee H, Park S et al. A recurrent inactivating mutation in RHOA GTPase in angioimmunoblastic T cell lymphoma. Nat Genet 2014; 46: 371–375.

44 Auguste T, Travert M, Tarte K, Ame-Thomas P, Artchounin C, Martin-Garcia N et al. ROQUIN/RC3H1 alterations are not found in angioimmunoblastic T-cell lymphoma. PLoS One 2013; 8: e64536.

45 Ellyard JI, Chia T, Rodriguez-Pinilla SM, Martin JL, Hu X, Navarro-Gonzalez M et al. Heterozygosity for Roquinsan leads to angioimmunoblastic T-cell lymphoma-like tumors in mice. Blood 2012; 120: 812–821.

46 Vinuesa CG, Cook MC, Angelucci C, Athanasopoulos V, Rui L, Hill KM et al. A RING-type ubiquitin ligase family member required to repress follicular helper T cells and autoimmunity. Nature 2005; 435: 452–458.

47 Baron BW, Anastasi J, Montag A, Huo D, Baron RM, Karrison T et al. The human BCL6 transgene promotes the development of lymphomas in the mouse. Proc Natl Acad Sci USA 2004; 101: 14198–14203.

48 Busque L, Patel JP, Figueroa ME, Vasanthakumar A, Provost S, Hamilou Z et al. Recurrent somatic TET2 mutations in normal elderly individuals with clonal hematopoiesis. Nat Genet 2012; 44: 1179–1181.

49 Asmar F, Punj V, Christensen J, Pedersen MT, Pedersen A, Nielsen AB et al. Genome-wide profiling identifies a DNA methylation signature that associates with TET2 mutations in diffuse large B-cell lymphoma. Haematologica 2013; 98: 1912–1920.

50 Pastor WA, Pape UJ, Huang Y, Henderson HR, Lister R, Ko M et al. Genome-wide mapping of 5-hydroxymethylcytosine in embryonic stem cells. Nature 2011; 473: 394–397.

51 Kantarjian H, Oki Y, Garcia-Manero G, Huang X, O'Brien S, Cortes J et al. Results of a randomized study of 3 schedules of low-dose decitabine in higher-risk myelo-dysplastic syndrome and chronic myelomonocytic leukemia. Blood 2007; 109: 52–57.

52 Fenaux P, Mufti GJ, Hellstrom-Lindberg E, Santini V, Finelli C, Giagounidis A et al. Efficacy of azacitidine compared with that of conventional care regimens in the treatment of higher-risk myelodysplastic syndromes: a randomised, open-label, phase III study. Lancet Oncol 2009; 10: 223–232.

Supplementary Information accompanies this paper on Blood Cancer Journal website (http://www.nature.com/bcj)